

Efficient Computation of Shap Explanation Scores for Neural Network Classifiers via Knowledge Compilation

Leopoldo Bertossi^{1*} and Jorge E. León^{2**}

¹ SKEMA Business School, Montreal, Canada

² Universidad Adolfo Ibáñez (UAI), Santiago, Chile

Abstract. The use of **Shap** scores has become widespread in Explainable AI. However, their computation is in general intractable, in particular when done with a black-box classifier, such as neural network. Recent research has unveiled classes of open-box Boolean Circuit classifiers for which **Shap** can be computed efficiently. We show how to transform binary neural networks into those circuits for efficient **Shap** computation. We use logic-based knowledge compilation techniques. The performance gain is huge, as we show in the light of our experiments.

1 Introduction

In recent years, there has been a growing demand for methods to explain and interpret the results from machine learning (ML) models. Explanations come in different forms, and can be obtained through different approaches. A common one assigns *attribution scores* to the features values associated to an input that goes through an ML-based model, to *quantify* their relevance for the obtained outcome. We concentrate on *local* scores, i.e. associated to a particular input, as opposed to a global score that indicated the overall relevance of a feature. We also concentrate on explanations for binary classification models that assign labels 0 or 1 to inputs.

A popular local score is **Shap** [16], which is based on the Shapley value that was introduced in coalition game theory and practice [29, 27]. **Shap** scores can be computed with a black-box or an open-box model [28]. With the former, we do not know or use its internal components, but only its input/output relation. This is the most common approach. In the latter case, we can have access to its internal structure and components, and we can use them for score computation. It is common to consider neural-network-based models as black-box models, because their internal gates and structure may be difficult to understand or process when it comes to explaining classification outputs. However, a decision-tree model, due to its much simpler structure and use, is considered to be open-box for the same purpose.

Even for binary classification models, the complexity of **Shap** computation is provably hard, actually $\#P$ -hard for several kinds of binary classification models, independently from whether the internal components of the model are used when computing **Shap** [3, 1, 2]. However, there are classes of classifiers for which, using the model components and structure, the complexity of **Shap** computation can be brought down to polynomial time [17, 2, 34].

* leopoldo.bertossi@skema.edu

** jorgleon@alumnos.uai.cl

A polynomial time algorithm for **Shap** computation with *deterministic and decomposable Boolean circuits* (dDBC_s) was presented in [2]. From this result, the tractability of **Shap** computation can be obtained for a variety of Boolean circuit-based classifiers and classifiers that can be represented as (or compiled into) them. In particular, this holds for *Ordered Binary Decision Diagrams* (OBDD_s) [7], decision trees, and other established classification models that can be compiled into (or treated as) OBDD_s [30, 10, 21]. This applies, in particular, to *Sentential Decision Diagrams* (SDD_s) [13] that form a convenient *knowledge compilation* target language [11, 33].

In this work, we show how to use logic-based knowledge compilation techniques to attack, and -to the best of our knowledge- for the first time, the important and timely problem of efficiently computing explanations scores in ML, which, without these techniques, would stay intractable.

More precisely, we concentrate on explicitly developing the compilation-based approach to the computation of **Shap** for *binary neural networks* (BNN_s). For this, a BNN is transformed into a dDBC using techniques from *knowledge compilation* [11], an area that investigates the transformation of (usually) propositional theories into an equivalent one with a canonical syntactic form that has some good computational properties, e.g. tractable model counting. The compilation may incur in a relatively high computational cost [11, 12], but it may still be worth the effort when a particular property is checked often, as is the case of explanations for the same BNN.

More specifically, we describe in detail how a BNN is first compiled into a propositional formula in Conjunctive Normal Form (CNF), which, in its turn, is compiled into an SDD, which is finally compiled into a dDBC. Our method applies at some steps established transformations that are not commonly illustrated or discussed in the context of real applications, which we do here. The whole compilation path so as the application to **Shap** computation are new. We show how **Shap** is computed on the resulting circuit via the efficient algorithm in [2]. This compilation is performed once, and is independent from any input to the classifier. The final circuit can be used to compute **Shap** scores for different input entities.

We also make experimental comparisons of computation times between this open-box and circuit-based **Shap** computation, and that based directly on the BNN treated as a black-box, i.e. using only its input/output relation. For our experiments, we consider real estate as an application domain, where house prices depend on certain features, which we appropriately binarize.³ The problem consists in classifying property blocks, represented as entity records of thirteen feature values, as *high-value* or *low-value*, a binary classification problem for which a BNN is used.

To the best of our knowledge, our work is the first at using knowledge compilation techniques for efficiently computing **Shap** scores, and the first at reporting experiments with the polynomial time algorithms for **Shap** computation on binary circuits. We confirm that **Shap** computation via the dDBC vastly outperforms the direct **Shap** computation on the BNN. It is also the case that the scores obtained are fully aligned, as expected since the dDBC represents the BNN. The same probability distribution associated to the Shapley value is used with all the models.

³ California Housing Prices dataset: <https://www.kaggle.com/datasets/camnugent/california-housing-prices>.

Compilation of BNNs into OBDDs was done in [30, 10] for other purposes, not for **Shap** computation or any other kind of attribution score. In this work we concentrate only on explanations based on **Shap** scores. There are several other explanations mechanisms for ML-based classification and decision systems in general, and also specific for neural networks. See [15] and [26] for surveys.

This paper is structured as follows. Section 2 contains background on **Shap** and Boolean circuits (BCs). Section 3 shows in detail, by means of a running example, the kind of compilation of BNNs into dDBCs we use for the experiments. Section 4 presents the experimental setup, and the results of our experiments with **Shap** computation. In Section 5 we draw some conclusions.

2 Preliminaries

In coalition game theory and its applications, the Shapley value is a established measure of the contribution of a player to a shared wealth that is modeled as a game function. Given a set of players S , and a game function $G : \mathcal{P}(S) \rightarrow \mathbb{R}$, mapping subsets of players to real numbers, the Shapley value for a player $p \in S$ quantifies its contribution to G . It emerges as the only measure that enjoys certain desired properties [27]. In order to apply the Shapley value, one has to define an appropriate game function.

Now, consider a fixed entity $\mathbf{e} = \langle F_1(\mathbf{e}), \dots, F_N(\mathbf{e}) \rangle$ subject to classification. It has values $F_i(\mathbf{e})$ for features in $\mathcal{F} = \{F_1, \dots, F_N\}$. These values are 0 or 1 for binary features. In [16, 17], the Shapley value is applied with \mathcal{F} as the set of players, and with the game function $\mathcal{G}_{\mathbf{e}}(s) := \mathbb{E}(L(\mathbf{e}') \mid \mathbf{e}'_s = \mathbf{e}_s)$, giving rise to the **Shap** score. Here, $s \subseteq \mathcal{F}$, and \mathbf{e}_s is the projection (or restriction) of \mathbf{e} on (to) the s . The label function L of the classifier assigns values 0 or 1. The \mathbf{e}' inside the expected value is an entity whose values coincides with those of \mathbf{e} for the features in s . For feature $F \in \mathcal{F}$:

$$\begin{aligned} \text{Shap}(\mathcal{F}, \mathcal{G}_{\mathbf{e}}, F) = \sum_{s \subseteq \mathcal{F} \setminus \{F\}} \frac{|s|!(|\mathcal{F}| - |s| - 1)!}{|\mathcal{F}|!} [& \\ & \mathbb{E}(L(\mathbf{e}') \mid \mathbf{e}'_{s \cup \{F\}} = \mathbf{e}_{s \cup \{F\}}) - \mathbb{E}(L(\mathbf{e}') \mid \mathbf{e}'_s = \mathbf{e}_s)]. \end{aligned} \quad (1)$$

The expected value assumes an underlying probability distribution on the entity population. **Shap** quantifies the contribution of feature value $F(\mathbf{e})$ to the outcome label.

In order to compute **Shap**, we only need function L , and none of the internal components of the classifier. Given that all possible subsets of features appear in its definition, **Shap** is bound to be hard to compute. Actually, for some classifiers, its computation may become $\#P$ -hard [2]. However, in [2], it is shown that **Shap** can be computed in polynomial time for every *deterministic and decomposable Boolean circuit* (dDBC) used as a classifier. The circuit's internal structure is used in the computation.

Figure 1 shows a Boolean circuit that can be used as a binary classifier, with binary features x_1, x_2, x_3 , whose values are input at the bottom nodes, and then propagated upwards through the Boolean gates. The binary label is read off from the top node. This circuit is *deterministic* in that, for every \vee -gate, at most one of its inputs is 1 when the output is 1. It is *decomposable* in that, for every \wedge -gate, the inputs do not share features. The dDBC in the Figure is also *smooth*, in that sub-circuits that feed a same \vee -gate share the same features. It has a *fan-in* at most two, in that every \wedge -gate and \vee -gate have at most two inputs. We denote this subclass of dDBCs with dDBCSFi(2).

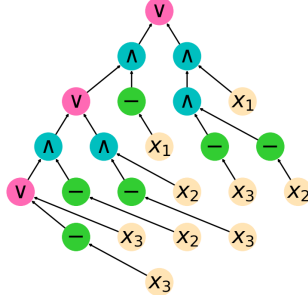


Fig. 1: A dDBC.

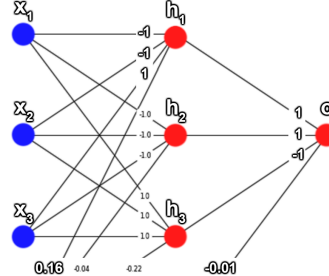


Fig. 2: A BNN.

More specifically, in [2] it is established that **Shap** can be computed in polynomial time for dDBCSFi(2)-classifiers, assuming that the underlying probability distribution is the uniform, P^u , or the product distribution, P^\times . They are as follows for binary features: $P^u(\mathbf{e}) := \frac{1}{2^N}$ and $P^\times(\mathbf{e}) := \prod_{i=1}^N p_i(F_i(\mathbf{e}))$, where $p_i(v)$ is the probability of value $v \in \{0, 1\}$ for feature F_i .

3 Compiling BNNs into dDBCs

In order to compute **Shap** with a BNN, we convert the latter into a dDBC, on which **Shap** scores will be computed with the polynomial time algorithm in [2]. The transformation goes along the the following path that we describe in this section:

$$\text{BNN} \xrightarrow{\text{(a)}} \text{CNF} \xrightarrow{\text{(b)}} \text{SDD} \xrightarrow{\text{(c)}} \text{dDBC} \quad (2)$$

A BNN can be converted into a CNF formula [31, 21], which, in its turn, can be converted into an SDD [13, 23]. It is also known that SDDs can be compiled into a formula in d-DNNF (deterministic and decomposable negated normal form) [11], which forms a subclass of dDBCs. More precisely, the resulting dDBC in (2) is finally compiled in polynomial time into a dDBCSFi(2).

Some of the steps in (2) may not be polynomial-time transformations, which we will discuss in more technical terms later in this section. However, we can claim at this stage that: (a) Any exponential cost of a transformation is kept under control by a usually small parameter. (b) The resulting dDBCSFi(2) is meant to be used multiple times, to explain different and multiple outcomes; and then, it may be worth taking a one-time, relatively high transformation cost. A good reason for our transformation path is the availability of implementations we can take advantage of.⁴

We will describe, explain and illustrate the conversion path (2) by means of a running example with a simple BNN, which is not the BNN used for our experiments. For them, we used a BNN with one hidden layer with 13 gates.

Example 1 The BNN in Figure 2 has hidden neuron gates h_1, h_2, h_3 , an output gate o , and three input gates, x_1, x_2, x_3 , that receive binary values. The latter represent,

⁴ The path in (2) is not the only way to obtain a dDBC. For example, [30] describe a conversion of BNNs into OBDDs, which can also be used to obtain dDBCs. However, the asymptotic time complexity is basically the same.

together, an input entity $\bar{x} = \langle x_1, x_2, x_3 \rangle$ that is being classified by means of a label returned by o . Each gate g is activated by means of a *step function* $\phi_g(\bar{i})$ of the form:

$$sp(\bar{w}_g \bullet \bar{i} + b_g) := \begin{cases} 1 & \text{if } \bar{w}_g \bullet \bar{i} + b_g \geq 0, \\ -1 & \text{otherwise and } g \text{ is hidden,} \\ 0 & \text{otherwise and } g \text{ is output,} \end{cases} \quad (3)$$

which is parameterized by a vector of binary weights \bar{w}_g and a real-valued constant bias b_g .⁵ The \bullet is the inner vector product. For technical, non-essential reasons, for a hidden gate, g , we use 1 and -1 , instead of 1 and 0, in \bar{w}_g and outputs. Similarly, $\bar{x} \in \{-1, 1\}^3$. Furthermore, we assume we have a single output gate, for which the activation function does return 1 or 0, for *true* or *false*, respectively.

For example, h_1 is *true*, i.e. outputs 1, for an input $\bar{x} = (x_1, x_2, x_3)$ iff $\bar{w}_{h_1} \bullet \bar{x} + b_{h_1} = (-1) \times x_1 + (-1) \times x_2 + 1 \times x_3 + 0.16 \geq 0$. Otherwise, h_1 is *false*, i.e. it returns -1 . Similarly, output gate o is *true*, i.e. returns label 1 for a binary input $\bar{h} = (h_1, h_3, h_3)$ iff $\bar{w}_o \bullet \bar{h} = 1 \times h_1 + 1 \times h_2 + (-1) \times h_3 - 0.01 \geq 0$, and 0 otherwise. \square

The first step, (a) in (2), represents the BNN as a CNF formula, i.e. as a conjunction of disjunctions of *literals*, i.e. atomic formulas or their negations.

Each gate of the BNN is represented by a propositional formula, initially not necessarily in CNF, which, in its turn, is used as one of the inputs to gates next to the right. In this way, we eventually obtain a defining formula for the output gate. The formula is converted into CNF. The participating propositional variables are logically treated as *true* or *false*, even if they take numerical values 1 or -1 , resp.

3.1 Representing BNNs as Formulas in CNF

Our conversion of the BNN into a CNF formula is inspired by a technique introduced in [21], in their case, to verify properties of BNNs. It cannot be applied straightforwardly in our setting since it introduces auxiliary variables, whose final elimination complicates the construction of the final BC. More precisely, the application of *variable forgetting* techniques [24] turn out to compromise the required determinism of the final circuit. In the following we describe a transformation that avoids introducing auxiliary variables.⁶ However, before describing the method in general, we give an example, to convey the main ideas and intuitions.

Example 2 (example 1 cont.) Consider gate h_1 , with parameters $\bar{w} = \langle -1, -1, 1 \rangle$ and $b = 0.16$, and input $\bar{i} = \langle x_1, x_2, x_3 \rangle$. An input x_j is said to be *conveniently instantiated* if it has the same sign as w_j , and then, contributing to having a larger number on the LHS of the comparison in (3). E.g., this is the case of $x_1 = -1$. In order to represent as a propositional formula its output variable, also denoted with h_1 , we first compute the number, d , of conveniently instantiated inputs that are necessary and sufficient to make the LHS of the comparison in (3) greater than or equal to 0. This is the (only) case when h_1 becomes *true*; otherwise, it is *false*. This number can be computed in general by [21]:

$$d = \left\lceil \left(-b + \sum_{j=1}^{|\bar{i}|} w_j \right) / 2 \right\rceil + \# \text{ of negative weights in } \bar{w}. \quad (4)$$

⁵ We could also used binarized *sigmoid* and *softmax* functions.

⁶ At this point is where using $1, -1$ in the BNN instead of $1, 0$ becomes useful.

For h_1 , with 2 negative weights: $d = \lceil (-0.16 + (-1 - 1 + 1))/2 \rceil + 2 = 2$. With this, we can impose conditions on two input variables with the right sign at a time, considering all possible convenient pairs. For h_1 we obtain its condition to be true:

$$h_1 \longleftrightarrow (-x_1 \wedge -x_2) \vee (-x_1 \wedge x_3) \vee (-x_2 \wedge x_3). \quad (5)$$

This DNF formula is directly obtained -and just to convey the intuition- from considering all possible convenient pairs (which is already better than trying all cases of three variables at a time). However, the general iterative method presented later in this subsection, is more expedite and compact than simply listing all possible cases; and still uses the number of convenient inputs. Using this general algorithm, we obtain, instead of (5), this equivalent formula defining h_1 :

$$h_1 \longleftrightarrow (x_3 \wedge (-x_2 \vee -x_1)) \vee (-x_2 \wedge -x_1). \quad (6)$$

Similarly, we obtain defining formulas for h_2 , h_3 , and o : (for all of them, $d = 2$)

$$\begin{aligned} h_2 &\longleftrightarrow (-x_3 \wedge (-x_2 \vee -x_1)) \vee (-x_2 \wedge -x_1), \\ h_3 &\longleftrightarrow (x_3 \wedge (x_2 \vee x_1)) \vee (x_2 \wedge x_1), \\ o &\longleftrightarrow (-h_3 \wedge (h_2 \vee h_1)) \vee (h_2 \wedge h_1). \end{aligned} \quad (7)$$

Replacing the definitions of h_1 , h_2 , h_3 into (7), we finally obtain:

$$\begin{aligned} o \longleftrightarrow & (-[(x_3 \wedge (x_2 \vee x_1)) \vee (x_2 \wedge x_1)] \wedge ([-(x_3 \wedge (-x_2 \vee -x_1)) \vee (-x_2 \wedge -x_1)] \\ & \vee [(x_3 \wedge (-x_2 \vee -x_1)) \vee (-x_2 \wedge -x_1)])) \vee ([-(x_3 \wedge (-x_2 \vee -x_1)) \vee \\ & (-x_2 \wedge -x_1)] \wedge [(x_3 \wedge (-x_2 \vee -x_1)) \vee (-x_2 \wedge -x_1)]). \end{aligned} \quad (8)$$

The final part of step (a) in path (2), requires transforming this formula into CNF. In this example, it can be taken straightforwardly into CNF. For our experiments, we implemented and used the general algorithm presented right after this example. It guarantees that the generated CNF formula does not grow unnecessarily by eliminating some redundancies along the process. The resulting CNF formula is, in its turn, simplified into a shorter and simpler new CNF formula by means of the *Confer* SAT solver [18]. For this example, the simplified CNF formula is as follows:

$$o \longleftrightarrow (-x_1 \vee -x_2) \wedge (-x_1 \vee -x_3) \wedge (-x_2 \vee -x_3). \quad (9)$$

Having a CNF formula will be convenient for the next steps along path (2). \square

In more general terms, consider a BNN receiving ℓ_0 input features, say $\bar{x} = \langle x_1, \dots, x_{\ell_0} \rangle$, and with m hidden layers z (from 1 to m), with ℓ_z neurons. A neuron in layer z receives the input vector $\bar{i} = \langle i_1, \dots, i_{\ell_{z-1}} \rangle$. The output layer has a single neuron.

To convert the BNN into a CNF formula, we do it layerwise from input to output. All the neurons in a layer can be converted in parallel. For every neuron gate g , we encode the case when it returns 1, representing its activation function $sp(\bar{w}_g \bullet \bar{i} + b_g)$ as a CNF formula. For this, we compute, as in (4), the number d_g of inputs to be instantiated for the output to be 1.

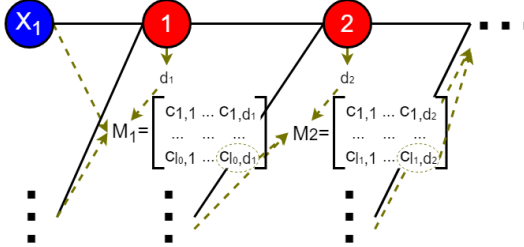


Fig. 3: From BNN to CNF (fragment). Initial variables (in blue) are inputs for first layer. Neurons ① and ② (in red) have d_1, d_2 and arrays M_1, M_2 , whose bottom, right entries encode ① and ②, resp. They are given as inputs to the arrays for the next layer.

For each neuron g on the first layer, and to conveniently manage the whole process, we construct a matrix-like structure M_g of dimension $|\bar{i}| \times d_g$, whose components $c_{k,t}$ are propositional formulas:

$$M_g = \begin{bmatrix} w_1 \cdot i_1 & \text{false} & \text{false} & \dots & \text{false} \\ w_2 \cdot i_2 & w_2 \cdot i_2 & \text{false} & \dots & \text{false} \\ \vee c_{1,1} & \wedge c_{1,1} & & & \\ w_3 \cdot i_3 & (w_3 \cdot i_3 \wedge c_{2,1}) & w_3 \cdot i_3 & \dots & \text{false} \\ \vee c_{2,1} & \vee c_{2,2} & \wedge c_{2,2} & & \\ \dots & \dots & \dots & \dots & \dots \\ w_{|\bar{i}|} \cdot i_{|\bar{i}|} \vee c_{|\bar{i}|-1,1} & (w_{|\bar{i}|} \cdot i_{|\bar{i}|} \wedge c_{|\bar{i}|-1,1}) \vee c_{|\bar{i}|-1,2} & (w_{|\bar{i}|} \cdot i_{|\bar{i}|} \wedge c_{|\bar{i}|-1,2}) \vee c_{|\bar{i}|-1,3} & \dots & c_{|\bar{i}|-1, d_g-1} \vee c_{|\bar{i}|-1, d_g} \end{bmatrix}$$

In it, a term of the form $w_k \cdot i_k$ does not represent a number, but a propositional formula, namely i_k if $w_k = 1$, and $\neg i_k$ if $w_k = -1$. Every M_g is filled in a row-wise manner starting from the top, and then column-wise from left to right. The formula that will be passed over to the next layer to the right is the last, bottom-right entry, $c_{|\bar{i}| \times d_g}$.

Only in the arrays for the first layer we find new propositional variables, for the inputs. For the next layers, the whole output formulas from the previous layer are passed over as inputs, and they become the i_k 's just mentioned. In this way, no auxiliary variables other than those for the initial inputs are created. Each row represents the number of the first $k \in \{1, \dots, |\bar{i}|\}$ inputs considered for the encoding, and each column, the threshold $t \in \{1, \dots, d_g\}$ to surpass (meaning that at least t inputs should be instantiated conveniently). For every component where $k < t$, the threshold cannot be reached, which makes every component in the upper, right triangle to be *false*.

For explanation, the first row of M_g has the first entry $w_1 \cdot i_1$, and *false* for the rest. Each entry $c_{k,1}$ of the first column becomes $w_k \cdot i_k \vee c_{k-1,1}$. For any other component $c_{k,t}$, $t > 1$, we use $(w_k \cdot i_k \wedge c_{k-1,t-1}) \vee c_{k-1,t}$. So, the lower right component $c_{|\bar{i}|, d_g}$ of M_g ends up being the encoding of neuron g , and it is the only formula that will be used in the encodings for the next layer. All the M_g 's for a layer can be generated in parallel, as their encodings do not influence each other.

For the second layer, we take as inputs the encodings c_{ℓ_0, d_g} from the previous one, and we keep repeating this conversion. In other words, we compute d_g and M_g for every neuron g in the new layer, taking the previous encodings as inputs. The resulting c_{ℓ_1, d_g} 's are given as inputs for the next layer, and we iterate all the way until the last layer. For illustration, see Figure 3.

From the array M_o for the single output neuron, o , at the last layer, we extract the component c_{ℓ_m, d_o} , which becomes the propositional encoding of the whole BNN. This is a propositional formula that is next converted into a CNF formula, which in its turn is further simplified (see Example 2). Actually, every entry in the array M_g is immediately transformed into CNF and simplified, avoiding the iterative creation of extremely long, complex or non-CNF formulas.

Departing from [21], our use of the M_g arrays helps us obtain a final propositional formula that can be transformed into a deterministic BC. However, even with both methods running in quadratic time, ours is computationally more costly (as verified in our experiments, with our much perfectible implementations). This is due to the simplifications we make during the construction of the CNF, which are not necessary when auxiliary variables are used. The obtained CNF can be further simplified by means of a SAT solver, as we did. However, this is not mandatory for what follows next.

3.2 Building an SDD Along the Way

Following with step (b) along path (2), the resulting CNF formula is transformed into a *Sentential Decision Diagram* (SDD) [13, 33], which, as a particular kind of *decision diagram* [5], is a directed acyclic graph. So as the popular OBDDs [7], that SDDs generalize, they can be used to represent general Boolean formulas, in particular, propositional formulas (but without necessarily being *per se* propositional formulas).

Example 3 (example 2 cont.) Figure 4(a) shows an SDD, \mathcal{S} , representing our CNF formula on the RHS of (9). An SDD has different kinds of nodes. Those represented with encircled numbers are *decision nodes* [33], e.g. ① and ③, that consider alternatives for the inputs (in essence, disjunctions). There are also nodes called *elements*. They are labeled with constructs of the form $[\ell_1|\ell_2]$, where ℓ_1, ℓ_2 , called the *prime* and the *sub*, resp., are Boolean literals, e.g. x_1 and $\neg x_2$, including \top and \perp , for 1 or 0, resp. E.g. $[\neg x_2|\top]$ is one of them. The *sub* can also be a pointer, \bullet , with an edge to a decision node. $[\ell_1|\ell_2]$ represents two conditions that have to be satisfied simultaneously (in essence, a conjunction). An element without \bullet is a *terminal*. (See [6, 20] for a precise definition of SDD.)

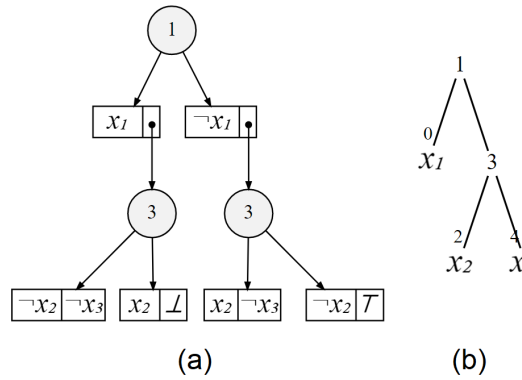


Fig. 4: An SDD (a) and a vtree (b).

An SDD represents (or defines) a total Boolean function $F_S: \langle x_1, x_2, x_3 \rangle \in \{0, 1\}^3 \mapsto \{0, 1\}$. For example, $F_S(0, 1, 1)$ is evaluated by following the graph downwards. Since

$x_1 = 0$, we descent to the right; next via node ③ underneath, with $x_2 = 1$, we reach the instantiated leaf node labeled with $[1|0]$, a “conjunction”, with the second component due to $x_3 = 1$. We obtain $F_S(0, 1, 1) = 0$. \square

In SDDs, the orders of occurrence of variables in the diagram must be compliant with a so-called *vtree* (for “variable tree”).⁷ The connection between a vtree and an SDD refers to the compatibility between the partitions $[prime|sub]$ and the tree structure (see Example 4 below). Depending on the chosen vtree, substructures of an SDD can be better reused when representing a Boolean function, e.g. a propositional formula, which becomes important to obtain a compact representation. SDDs can easily be combined via propositional operations, resulting in a new SDD [13].

A vtree for a set of variables \mathcal{V} is binary tree that is full, i.e. every node has 0 or 2 children, and ordered, i.e. the children of a node are totally ordered, and there is a bijection between the set of leaves and \mathcal{V} [6].

Example 4 (example 3 cont.) Figure 4(b) shows a vtree, \mathcal{T} , for $\mathcal{V} = \{x_1, x_2, x_3\}$. Its leaves, 0, 2, 4, show their associated variables in \mathcal{V} . The SDD S in Figure 4(a) is compatible with \mathcal{T} . Intuitively, the variables at S ’s terminals, when they go upwards through decision nodes \mathcal{n} , also go upwards through the corresponding nodes n in \mathcal{T} . (See [6, 20, 5] for a precise, recursive definition.)

The SDD S can be straightforwardly represented as a propositional formula by interpreting decision points as disjunctions, and elements as conjunctions, obtaining $[x_1 \wedge ((-x_2 \wedge -x_3) \vee (x_2 \wedge \perp))] \vee [-x_1 \wedge ((x_2 \wedge -x_3) \vee (-x_2 \wedge \top))]$, which is logically equivalent to the formula on the RHS of (9) that represents our BNN. \square

For the running example and experiments, we used the *PySDD* system [19]: Given a CNF formula ψ , it computes an associated vtree and a compliant SDD, both optimized in size [8, 9]. This compilation step, the theoretically most expensive along path (2), takes exponential space and time only in $TW(\psi)$, the *tree-width* of the graph \mathcal{G} associated to ψ [13, 23]. \mathcal{G} contains the variables as nodes, and undirected edges between any of them when they appear in a same clause. The tree-width measures how close the graph is to being a tree. This is a positive *fixed-parameter tractability* result [14], in that $TW(\psi)$ is in general smaller than $|\psi|$. For example, the graph \mathcal{G} for the formula ψ on the RHS of (9) has x_1, x_2, x_3 as nodes, and edges between any pair of variables, which makes \mathcal{G} a complete graph. Since every complete graph has a tree-width equal to the number of nodes minus one, we have $TW(\psi) = 2$.

3.3 The Final dDBC

Our final dDBC is obtained from the resulting SDD: An SDD corresponds to a d-DNNF Boolean circuit, for which decomposability and determinism hold, and has only variables as inputs to negation gates [13]. d-DNNFs are also dDBCs.

The algorithm in [2] for *Shap* computation needs the dDBC to be a dDBCSFi(2), whose computation we describe next. Algorithm 1 does this job. In a bottom-up fashion, fan-in 2 is achieved by rewriting every \wedge -gate (resp., and \vee -gate) of fan-in $m > 2$

⁷ Extending OBDDs, whose vtrees make variables in a path always appear in the same order. This generalization makes SDDs much more succinct than OBDDs [33, 6, 5].

with a chain of $m - 1$ \wedge -gates (resp., \vee -gates) of fan-in 2. After that, to enforce smoothness, for every disjunction gate (now with a fan-in 2) of subcircuits C_1 and C_2 , find the set of variables in C_1 , but not in C_2 (denoted V_{1-2}), along with those in C_2 , but not in C_1 (denoted V_{2-1}). For every variable $v \in V_{2-1}$, redefine C_1 as $C_1 \wedge (v \vee \neg v)$. Similarly, for every variable $v \in V_{1-2}$, redefine C_2 as $C_2 \wedge (v \vee \neg v)$. For example, for $(x_1 \wedge x_2 \wedge x_3) \vee (x_2 \wedge \neg x_3)$, becomes $((x_1 \wedge x_2) \wedge x_3) \vee ((x_2 \wedge \neg x_3) \wedge (x_1 \vee \neg x_1))$. Since this transformation visits each node once, the time complexity is linear in the number of nodes of the dDBC.

Algorithm 1: From dDBC to dDBCSFi(2)

Input : Original dDBC (starting from root node).
Output: A dDBCSFi(2) equivalent to the given dDBC.

```

1 function FIX_NODE(dDBC_node)
2   if dDBC_node is a disjunction then
3     |    $c_{new} = \text{false}$ 
4     |   for each subcircuit  $sc$  in dDBC_node
5       |     |    $sc_{fixed} = \text{FIX\_NODE}(sc)$ 
6       |     |   if  $sc_{fixed}$  is a true value or is equal to  $\neg c_{new}$  then
7         |       |   return true
8       |     |   else if  $sc_{fixed}$  is not a false value then
9         |       |     |   for each variable  $v$  in  $c_{new}$  and not in  $sc_{fixed}$ 
10        |         |       |    $| sc_{fixed} = sc_{fixed} \wedge (v \vee \neg v)$ 
11        |       |     |   for each variable  $v$  in  $sc_{fixed}$  and not in  $c_{new}$ 
12        |         |       |    $| c_{new} = c_{new} \wedge (v \vee \neg v)$ 
13        |       |    $c_{new} = c_{new} \vee sc_{fixed}$ 
14     |   return  $c_{new}$ 
15   else if dDBC_node is a conjunction then
16     |    $c_{new} = \text{true}$ 
17     |   for each subcircuit  $sc$  in dDBC_node
18       |     |    $sc_{fixed} = \text{FIX\_NODE}(sc)$ 
19       |     |   if  $sc_{fixed}$  is a false value or is equal to  $\neg c_{new}$  then
20         |       |   return false
21       |     |   else if  $sc_{fixed}$  is not a true value then
22         |       |    $c_{new} = c_{new} \wedge sc_{fixed}$ 
23     |   return  $c_{new}$ 
24   else if dDBC_node is a negation then
25     |   return  $\neg \text{FIX\_NODE}(\neg dDBC\_node)$ 
26   else
27     |   return dDBC_node
28  $dDBCSFi(2) = \text{FIX\_NODE}(\text{root\_node})$ 

```

Example 5 (example 3 cont.) By interpreting decision points and elements as disjunctions and conjunctions, resp., the SDD in Figure 4(a) can be easily converted into d-DNNF circuit. Only variables are affected by negations. Due to the children of node ③, that do not have the same variables, the resulting dBBC is not smooth (but it has fan-in 2). Algorithm 1 transforms it into the dDBCSFi(2) in Figure 1. \square

4 Shap Computation: Experiments

The “California Housing Prices” dataset was used for our experiments (it can be downloaded from Kaggle [22]). It consists of 20,640 observations for 10 features with information on the block groups of houses in California, from the 1990 Census. Table 1 lists and describes the features, and the way they are binarized. The categorical feature #1 is one-hot encoded, giving rise to 5 binary features: $\#1_a, \dots, \#1_e$. Accordingly, we end up with 13 binary input features, plus the binary output feature, #10, representing whether the median price at each block is high or low, i.e. above or below the average of the original #10. We used the “Tensorflow” and “Larq” Python libraries to train a BNN with one hidden layer, with as many neurons as predictors, i.e. 13, and one neuron for the output. For the hidden neurons, the activation functions are step function, as in (3).

Table 1: Features of the “California Housing Prices” dataset.

Id #	Feature Name	Description	Original Values	Binarization
#1	<i>ocean_proximity</i>	A label of the location of the house w.r.t sea/ocean	Labels <i>1h_ocean, inland, island, near_bay</i> and <i>near_ocean</i>	Five features (one representing each label), for which 1 means a match with the value of <i>ocean_proximity</i> , and -1 otherwise
#2	<i>households</i>	The total number of households (a group of people residing within a home unit) for a block	Integer numbers from 1 to 6,082	1 (above average of the feature) or -1 (below average)
#3	<i>housing_median_age</i>	The median age of a house within a block (lower numbers means newer buildings)	Integer numbers from 1 to 52	1 (above average of the feature) or -1 (below average)
#4	<i>latitude</i>	The angular measure of how far north a block is (the higher value, the farther north)	Real numbers from 32.54 to 41.95	1 (above average of the feature) or -1 (below average)
#5	<i>longitude</i>	The angular measure of how far west a block is (the higher value, the farther west)	Real numbers from -124.35 to -114.31	1 (above average of the feature) or -1 (below average)
#6	<i>median_income</i>	The median income for households within a block (measured in tens of thousands of US dollars)	Real numbers from 0.50 to 15.00	1 (above average of the feature) or -1 (below average)
#7	<i>population</i>	The total number of people residing within a block	Integer numbers from 3 to 35,682	1 (above average of the feature) or -1 (below average)
#8	<i>total_bedrooms</i>	The total number of bedrooms within a block	Integer numbers from 1 to 6,445	1 (above average of the feature) or -1 (below average)
#9	<i>total_rooms</i>	The total number of rooms within a block	Integer numbers from 2 to 39,320	1 (above average of the feature) or -1 (below average)

Id #	Output	Description	Original Values	Labels
#10	<i>median_house_value</i>	The median house value for households within a block (measured in US dollars)	Integer numbers from 14,999 to 500,001	1 (above average of the feature) or 0 (below average)

According to the transformation path (2), the constructed BNN was first represented as a CNF formula with 2,391 clauses. It has a tree-width of 12, which makes sense having a middle layer of 13 gates, each with all features as inputs. The CNF was transformed, via the SDD conversion, into a dDBCSFi(2), \mathcal{C} , which ended up having 18,671 nodes (without counting the negations affecting only input gates). Both transformations were programmed in Python. For the intermediate simplification of the CNF, the *Riss* SAT solver was used [18]. The initial transformation into CNF took 1.3 hrs. This is

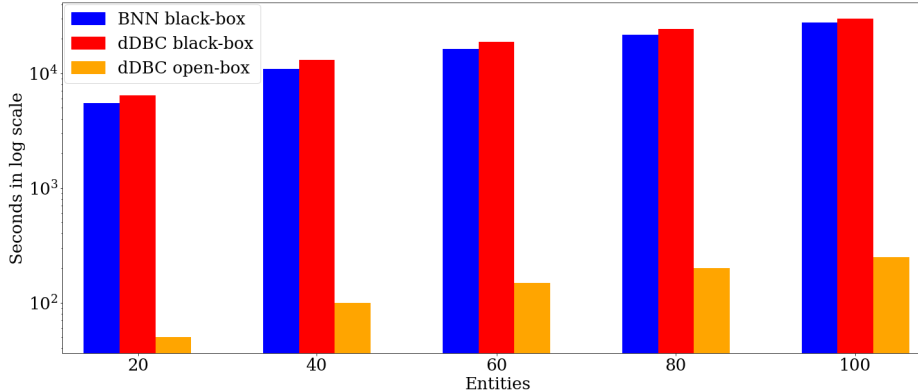


Fig. 5: Seconds taken to compute all **Shap** scores on 20, 40, 60, 80 and 100 entities; using the BNN as a black-box (blue bar), the dDBC as a black-box (red bar), and the dDBC as an open-box (orange bar). Notice the logarithmic scale on the vertical axis.

the *practically* most expensive step, as was explained at the end of Section 3.1. The conversion of the simplified CNF into the dDBCSFi(2) took 0.8276 secs.

With the resulting BC, we computed **Shap**, for each input entity, in three ways:

- (a) Directly on the BNN as a black-box model, using formula (1) and its input/output relation for multiple calls;
- (b) Similarly, using the circuit \mathcal{C} as a black-box model; and
- (c) Using the efficient algorithm in [1, page 18] treating circuit \mathcal{C} as an open-box model.

These three computations of **Shap** scores were performed for sets of 20, 40, 60, 80, and 100 input entities, for *all* 13 features, and *all* entities in the set. In all cases, using the uniform distribution over population of size 2^{13} . Since the dDBC faithfully represents the BNN, we obtained exactly the same **Shap** scores under the modes of computation (a)-(c) above. The *total* computation times were compared. The results are shown in Figure 5. Notice that these times are represented *in logarithmic scale*. For example, with the BNN, the computation time of all **Shap** scores for 100 entities was 7.7 hrs, whereas with the open-box dDBC it was 4.2 min. We observe a huge gain in performance with the use of the efficient algorithm on the open-box dDBC. Those times do not show the one-time computation for the transformation of the BNN into the dDBC. If the latter was added, each red and orange bar would have an increase of 1.3 hrs. For reference, even considering this extra one-time computation, with the open-box approach on the dDBC we can still compute all of the **Shap** scores for 100 entities in less time than with the BNN with just 20 entities.⁸

For the cases (a) and (b) above, i.e. computations with black-box models, the classification labels were first computed for all entities in the population \mathcal{E} . Accordingly, when computing the **Shap** scores for a particular input entity e , the labels for all the other entities related to it via a subset of features S as specified by the game function were already precomputed. This allows to compute formula (1) much more efficiently.⁹

⁸ The experiments were run on *Google Colab* (with an NVIDIA Tesla T4 enabled). Algorithm 1 was programmed in Python. The complete code for *Google Colab* can be found at: <https://github.com/Jorvan758/dDBCSFi2>.

⁹ As done in [3], but with only the entity sample.

The specialized algorithm for (c) does not require this precomputation. The difference in time between the BNN and the black-box dDBC, cases (a) and (b), is due the fact that BNNs allow some batch processing for the label precomputation; with the dDBC it has to be done one by one.

5 Conclusions

We have showed in detail the practical use of logic-based knowledge compilation techniques in a real application scenario. Furthermore, we have applied them to the new and important problem of efficiently computing attribution scores for explainable ML. We have demonstrated the huge computational gain, by comparing **Shap** computation with a BNN classifier treated as an open-box vs. treating it as a black-box. The performance gain in **Shap** computation with the circuit exceeds by far both the compilation time and the **Shap** computation time for the BNN as a black-box classifier.

We emphasize that the effort invested in transforming the BNN into a dDBC is something we incur once. The resulting circuit can be used to obtain **Shap** scores multiple times, and for multiple inputs. Furthermore, the circuit can be used for other purposes, such as *verification* of general properties of the classifier [21, 10]. Despite the intrinsic complexity involved, there is much room for improving the algorithmic and implementation aspects of the BNN compilation. The same applies to the implementation of the efficient **Shap** computation algorithm.

We computed **Shap** scores using the uniform distribution on the entity population. There are a few issues to discuss in this regard. First, it is computationally costly to use it with a large number of features. One could use instead the *empirical distribution* associated to the dataset, as in [3] for black-box **Shap** computation. This would require appropriately modifying the applied algorithm, which is left for future work. Secondly, and more generally, the uniform distribution does not capture possible dependencies among features. The algorithm is still efficient with the *product distribution*, which also suffers from imposing feature independence (see [3] for a discussion of its empirical version and related issues). It would be interesting to explore to what extent other distributions could be used in combination with our efficient algorithm.

Independently from the algorithmic and implementation aspects of **Shap** computation, an important research problem is that of bringing *domain knowledge* or *domain semantics* into attribution scores and their computations, to obtain more meaningful and interpretable results. This additional knowledge could come, for example, in declarative terms, expressed as *logical constraints*. They could be used to appropriately modify the algorithm or the underlying distribution [4]. It is likely that domain knowledge can be more easily be brought into a score computation when it is done on a BC classifier.

In this work we have considered only binary NNs. It would be interesting to investigate to what extent our methods can be applied to non-binary NNs. It is not clear whether work on binarized NNs [25, 35, 32] would be a feasible way to go.

Acknowledgments: Special thanks to Arthur Choi, Andy Shih, Norbert Manthey, Maximilian Schleich and Adnan Darwiche, for their valuable help. Work was funded by ANID - Millennium Science Initiative Program - Code ICN17002; CENIA, FB210017 (Financiamiento Basal para Centros Científicos y Tecnológicos de Excelencia de ANID), Chile; and SKEMA. L. Bertossi is a Professor Emeritus at Carleton University, Canada.

References

- [1] Arenas, M.; Barceló, P.; Bertossi, L.; and Monet, M. On the Complexity of SHAP-Score-Based Explanations: Tractability via Knowledge Compilation and Non-Approximability Results. *Journal of Machine Learning Research*, 2023, 24(63):1-58. Extended version of [2].
- [2] Arenas, M.; Barceló, P.; Bertossi, L.; and Monet, M. The Tractability of SHAP-Score-Based Explanations for Classification over Deterministic and Decomposable Boolean Circuits. In *Proceedings of the 35th AAAI Conference on Artificial Intelligence*, 2021, 6670–6678.
- [3] Bertossi, L.; Li, J.; Schleich, M.; Suciu, D.; and Vagena, Z. Causality-Based Explanation of Classification Outcomes. In *Proceedings of the 4th International Workshop on "Data Management for End-to-End Machine Learning" (DEEM) at ACM SIGMOD/PODS*, 2020, 1–10. Posted as Corr ArXiv Paper 2003.06868.
- [4] Bertossi, L. Declarative Approaches to Counterfactual Explanations for Classification. *Theory and Practice of Logic Programming*, 2023, 23(3):559–593.
- [5] Bollig, B.; and Buttkus, M. On the Relative Succinctness of Sentential Decision Diagrams. *Theory of Computing Systems*, 2019, 63(6):1250–1277.
- [6] Bova, S. SDDs Are Exponentially More Succinct than OBDDs. In *Proceedings of the 30th AAAI Conference on Artificial Intelligence*, 2016, 929–935.
- [7] Bryant, R. E. Graph-Based Algorithms for Boolean Function Manipulation. *IEEE Transactions on Computers*, 1986, C-35(8):677–691.
- [8] Choi, A.; and Darwiche, A. Dynamic Minimization of Sentential Decision Diagrams. In *Proceedings of the 27th AAAI Conference on Artificial Intelligence*, 2013, 187–194.
- [9] Choi, A.; and Darwiche, A. *SDD Advanced-User Manual Version 2.0*, 2018. Automated Reasoning Group, UCLA.
- [10] Darwiche, A.; and Hirth, A. On The Reasons Behind Decisions. In *Proceedings of the 24th European Conference on Artificial Intelligence*, 2020, 712–720.
- [11] Darwiche, A.; and Marquis, P. A Knowledge Compilation Map. *Journal of Artificial Intelligence Research*, 2002, 17(1):229–264.
- [12] Darwiche, A. On the Tractable Counting of Theory Models and its Application to Truth Maintenance and Belief Revision. *Journal of Applied Non-Classical Logics*, 2011, 11(1-2):11–34.
- [13] Darwiche, A. SDD: A New Canonical Representation of Propositional Knowledge Bases. In *Proceedings of the 22th International Joint Conference on Artificial Intelligence (IJCAI-11)*, 2011, 819–826.
- [14] Flum, J.; and Grohe, M. *Parameterized Complexity Theory*, 2006. Springer.
- [15] Guidotti, R.; Monreale, A.; Ruggieri, S.; Turini, F.; Giannotti, F.; and Pedreschi, D. A Survey of Methods for Explaining Black Box Models. *ACM Computing Surveys*, 2018, 51(5):1–42.
- [16] Lundberg, S. M.; and Lee, S.-I. A Unified Approach to Interpreting Model Predictions. In *Proceedings of the 31st International Conference on Neural Information Processing Systems*, 2017, 4768–4777. ArXiv Paper 1705.07874.
- [17] Lundberg, S.; Erion, G.; Chen, H.; DeGrave, A.; Prutkin, J.; Nair, B.; Katz, R.; Himmelfarb, J.; Bansal, N.; and Lee, S.-I. From Local Explanations to Global Understanding with Explainable AI for Trees. *Nature Machine Intelligence*, 2020, 2(1):56–67. ArXiv Paper 1905.04610.
- [18] Manthey, N. Riss tool collection, 2017. <https://github.com/nmanthey/riss-solver>.
- [19] Meert, W.; and Choi, A. Python Wrapper Package to Interactively use Sentential Decision Diagrams (SDD), 2018. <https://github.com/wannesm/PySDD>.

[20] Nakamura, K.; Denzumi, S.; and Nishino, M. Variable Shift SDD: A More Succinct Sentential Decision Diagram. In *Proceedings of the 18th International Symposium on Experimental Algorithms (SEA 2020). Leibniz International Proceedings in Informatics 160*, 2020, 22:1–22:13.

[21] Narodytska, N.; Kasiviswanathan, S.; Ryzhyk, L.; Sagiv, M.; and Walsh, T. Verifying Properties of Binarized Deep Neural Networks. In *Proceedings of the 32nd AAAI Conference on Artificial Intelligence*, 2018, 6615–6624.

[22] Nugent, C. California Housing Prices, 2018. <https://www.kaggle.com/datasets/camnugent/california-housing-prices>.

[23] Oztok, U.; and Darwiche, A. On Compiling CNF into Decision-DNNF. In *Proceedings of the 20th International Conference on Principles and Practice of Constraint Programming, Lecture Notes in Computer Science 8656*, 2014, 42–57.

[24] Oztok, U.; and Darwiche, A. On Compiling DNNFs without Determinism, 2017. *ArXiv* 1709.07092.

[25] Qin, H.; Gong, R.; Liu, X.; Bai, X.; Song, J.; and Sebe, N. Binary Neural Networks: A Survey. *Pattern Recognition*, 2020, 105:107281.

[26] Ras, G.; Xie, N.; van Gerven, M.; and Doran, D. Explainable Deep Learning: A Field Guide for the Uninitiated. *Journal of Artificial Intelligence Research*, 2022, 73:329–396.

[27] Roth, A. *The Shapley Value: Essays in Honor of Lloyd S. Shapley*, 1988. Cambridge University Press.

[28] Rudin, C. Stop Explaining Black Box Machine Learning Models for High Stakes Decisions and Use Interpretable Models Instead. *Nature Machine Intelligence*, 2019, 1:206–215. ArXiv Paper 1811.10154.

[29] Shapley, L. S. A Value for n-Person Games. In *Contributions to the Theory of Games (AM-28)*, 1953, V. 2, 307–318.

[30] Shi, W.; Shih, A.; Darwiche, A.; and Choi, A. On Tractable Representations of Binary Neural Networks. In *Proceedings of the 17th International Conference on Principles of Knowledge Representation and Reasoning*, 2020, 882–892.

[31] Shih, A.; Darwiche, A.; and Choi, A. Verifying Binarized Neural Networks by Angluin-Style Learning. In *Proceedings of the Theory and Applications of Satisfiability Testing - SAT 2019, Lecture Notes in Computer Science 11628*, 2019, 354–370.

[32] Simons, T.; and Lee, D.-J. A Review of Binarized Neural Networks. *Electronics*, 2019, 8(6):661.

[33] Van den Broeck, G.; and Darwiche, A. On the Role of Canonicity in Knowledge Compilation. In *Proceedings of the 29th AAAI Conference on Artificial Intelligence*, 2015, 1641–1648.

[34] Van den Broeck, G.; Lykov, A.; Schleich, M.; and Suciu, D. On the Tractability of SHAP Explanations. In *Proceedings of the 35th AAAI Conference on Artificial Intelligence*, 2021, 6505–6513.

[35] Yuan, C.; and Agaian, S. S. 2021. A Comprehensive Review of Binary Neural Network, 2021. *ArXiv* 2110.06804.